

Wear Resistance and Mechanical Behaviour of Epoxy/Mollusk Shell Biocomposites developed for Structural Applications

I.O. Oladele^{a,d}, J.L. Olajide^{a,b,c}, M. Amujede^a

^aDepartment of Metallurgical and Materials Engineering, Federal university of Technology, Akure, Nigeria,

^bDepartment of Mechanical Engineering, Elizade University, Ilara-Mokin, Nigeria,

^cDivision of Computational Materials Science and Prototype Engineering Development, Quantum Simutech Enterprise, Ilorin, Nigeria,

^dAfrican Materials Science and Engineering Network (AMSEN) A Carnegie-IAS (RISE) Network, (FUTA Node) Akure, Nigeria.

Keywords:

*Sustainable materials
Industrial applications
Polymer tribology
Mechanical properties
Critical filler content*

ABSTRACT

Epoxy resin is one of the strongest commercially exploitable thermosetting polymers in the polymer family; however its expensive nature in comparison with other thermosetting polymers such as vinylester and polyester limits its applications as a structural material. Inexpensive fillers on the other hand, especially those derived from agro-industrial wastes are very important in reducing the overall cost of polymer composites and furthermore influential in enhancing some of their engineering properties. In the present study, the wear resistance and mechanical behaviour of epoxy polymer matrix filled with <75 and 75 μm calcined particles of African land snail shells have been comparatively investigated. The wear resistance and the mechanical behaviour of the composites were studied via Taber Abraser and INSTRON universal testing machine. Also, the elemental constituents of the calcined snail shell and the epoxy biocomposites were characterized by X-Ray Fluorescence Spectroscopy and Scanning Electron Microscopy/Energy Dispersion Spectroscopy. From the experimental results, it was observed that, at the highest filler loading, smaller particle size presented a biocomposite with significant enhancement in wear and mechanical properties. However, it was also observed that increase in particle size showed no significant enhancement in the mechanical properties of the biocomposites.

Corresponding author:

*I.O. Oladele
Department of Metallurgical and
Materials Engineering, Federal
university of Technology, Akure,
Nigeria.
E-mail: wolesuccess2000@yahoo.com*

© 2016 Published by Faculty of Engineering

1. INTRODUCTION

In recent times, it has become unreservedly imperative for every nation across the globe to

appreciably embrace every possible conduit of promoting environmental safety, due to the unremitting nature of severity that is now a predominant concomitance of the stringencies of

present environmental regulations. In agreement with the foregoing occurrence, concerned citizens around the world are intensely enjoined by global environmentalists to take participatory steps in promoting a safer and healthier environment [1,2]. In an appreciable response to the persistent entreaties of these environmentalists, concerned researchers around the world have preeminently promulgated the idea of integrating agro-industrial wastes such as avian feathers [3,4] mammalian hairs [5], mollusk shells [6], egg shells [7,8] dead animal bones [9,10] and vegetal fibres and fillers in contemporary composites [11,12]. Interestingly, this striking approach presents an economically viable way and a greener method of developing novel and sustainable engineering materials with versatile areas of applications. In addition, it appreciably supports the zero-waste itinerary of manufacturing processes.

As obtainable from existing literature, one of the abundantly exploitable wastes for the development of contemporary engineering materials is snail shell [13,14]. Snail shells primarily consist of calcium carbonate (CaCO_3) which happens to be a conventional mineral filler for composites development and this in turn, presents pulverized snail shell as a suitable and low-cost bioparticulate for the development of inexpensive and high-performance biocomposites [15,16].

Quite a remarkable number of investigations have been able to confidently establish that particulates derived from snail shells can be significantly used to enhance some of the inherent engineering properties of polymeric materials. Adeosun *et al.* [17] developed polyester composites with improved thermal properties with the addition of snail shells to polyester, Madueke *et al.* [18] reported improved mechanical behaviour of unsaturated polyester filled with snail shell particles, also the work of Onuegbu and Igwe [19] revealed an improvement in the mechanical behavior of polypropylene filled with varying particle sizes of snail shell powder.

In addition, a recent scientific report by Buranyi [20] markedly pointed out that biomimicry of the structure of the abalone snail shell according to ongoing research by researchers in McGill University's Laboratory for Advanced Materials and Bioinspiration in Canada and Leibniz

Institute for Interactive Materials Aachen in Germany, is definitely an inspirational postern to developing the toughest materials of the future.

However, in spite of all these noteworthy accomplishments, the use of snail shell ash as a biofiller in the development of epoxy biocomposites for structural applications has not been documented. The present study focused on developing low-cost epoxy/mollusk shell biocomposites (EMSBS) with improved wear and mechanical properties.

Epoxy resin is one of the strongest polymeric materials known to man with a lot of other attractive properties such as corrosion resistance, resistance to environmental degradation, ability to strongly adhere to a variety of substrates and an appreciable resistance to thermal decomposition in comparison with other thermosetting polymers [21]. However, these attractive properties rendered epoxy an expensive material which in turn has limited its areas of applications [22]. The predominant application of epoxy is seen in coating and structural applications account for the second largest share of epoxy resin consumption [23]. The prevalent structural applications of epoxy and their composites are principally seen in the monocues of race cars [24], wind energy and aerospace turbine blades [25], hulls and keels of boats [26] and flight support structures for spacecraft [27].

The background of the present research was established based on the intensifying need to reassess the economic importance of snail shells in Nigeria and the emergent need to expand the structural applications of epoxy resin within the circumference of economic viability, and opportunely, this could be achieved by replacing some of the expensive conventional reinforcing materials for epoxy composites such as carbon, graphite and Kevlar fibres with snail shell ash [28].

Snail shells constitute a principal source of environmental nuisance in Nigeria, as they are regarded as wastes and deposited in landfills after their edible parts have been removed. These shells do not decompose easily; according to Pearce [29] the decomposition rate of dead snail shells averaged 6.4 % per year. The shell of

the African land snail (*Achatina fulica*) was selected as the mollusk shell for the present study. *Achatina fulica* is one of the predominant species of snails in Nigeria and it is relatively abundant [30].

In the present study, the effect of particle size and filler loading on the abrasive wear resistance and mechanical behavior of epoxy resin filled with calcined particulate of African land snail shell were investigated.

2. MATERIALS AND METHODS

2.1 Materials

The materials used in this study were basically African land snail shells and Bisphenol-A, epoxy resin. The shells were sourced and acquired from food restaurants' scrapheap in Ikeja metropolis, Lagos state, Nigeria. The age of the snails from which the shells were acquired ranged between 4.5 years \pm 5 months. The epoxy resin and the amine hardener were supplied by Orkila chemicals Ltd, Ikeja, Lagos state, Nigeria.

2.2 Preparation of the Mollusk Shell Ash (MSA)

Removal of impurities from the shells was achieved by thoroughly washing them with flowing water and this was ensued by sun-drying them for 3 days at about 27 ± 2 °C. Consequently, the dried shells were transferred into a kiln heated at a constant temperature of 1000 °C for 2 hours to remove residual organic matters. Pulverization of the calcined shells was then carried out automatically by a pulverizing machine and this was ensued by sieving the pulverized shells with sieves having meshes of 75 μ m and <75 μ m, respectively.



Fig. 1. Photographic representations of (a) 75 μ m calcined MSA (b) <75 μ m calcined MSA.

The photographic representations of snail shells particles i.e. the fillers, after calcinations are presented in Fig. 1. Both particle sizes used as fillers in the biocomposites are shown.

The result of the X-Ray Fluorescence Spectroscopy (XRF) of the MSA is presented in (Table 1).

Table 1. XRF analysis result for the calcined MSA.

Element	Conc. Value [wt. %]	Conc. Error [\pm]
K	0.220	0.009
Ca	1.522	0.045
Ti	0.101	0.010
Mn	100	16
Ni	32	5
Fe	0.0002833	0.0000011
Zn	0.0029	0.0004
Ga	0.0013	0.0009
As	0.0003	0.0001
Rb	0.0014	0.0006
Sr	0.0044	0.001
Se	0.002	0.0005
Zr	0.0221	0.0031
V	0.0103	0.0017

2.3 Development of the Test Samples

The composites were produced through open-mould casting technique. A homogenous mixture of the MSA, the epoxy resin and the hardener was achieved via manual mixing with a glass rod stirrer for 2 minutes in a polymeric container. Prior to introduction of the homogeneous mixture into the respective moulds, the moulds were coated with a releasing agent to facilitate the ease of removal of test samples. The samples were allowed to cure in air at room temperature which ranged between 24 ± 2 °C. The compositions of the two sets of composites produced and their corresponding curing times are presented in Tables 2 and 3. Correspondingly, in Fig. 2, the photographic representations of the developed test samples are presented and in Fig. 3 the results of the Scanning Electron Microscopy (SEM)/Energy Dispersion Spectroscopy (EDS) of the 10 wt.% EMSBs sets selected as the representative samples for both sets of composites are presented.

Table 2. Composition and curing time of the Neat Epoxy (NE) and the EMSBs filled with 75 µm MSA.

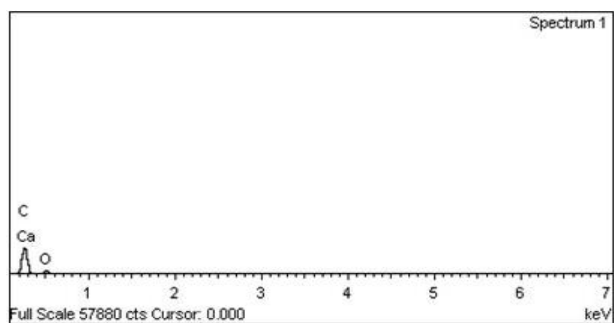
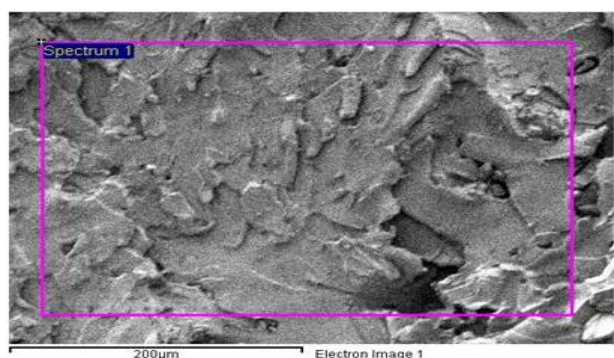
Sample designation	Weight of Epoxy (g)	Weight of MSA (g)	Epoxy (wt.%)	MSA (wt.%)	Curing time (hr)
NE	300	0	100	0	6:00
2 wt.%	294	6	98	2	5:00
4 wt.%	288	12	96	4	4:20
6 wt.%	282	18	94	6	3:45
8 wt.%	276	24	92	8	3:30
10 wt.%	270	30	90	10	3:20

Table 3. Composition and curing time of the NE and the EMSBs filled with <75 µm MSA.

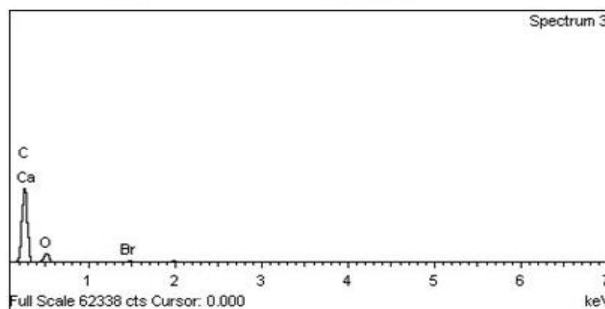
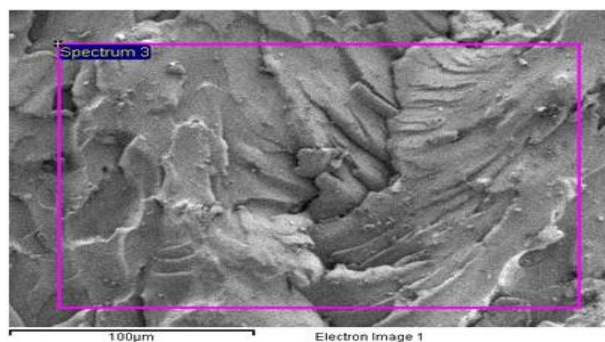
Sample designation	Weight of Epoxy (g)	Weight of MSA (g)	Epoxy (wt.%)	MSA (wt.%)	Curing time (hr)
NE	300	0	100	0	6:00
2 wt.%	294	6	98	2	4:40
4 wt.%	288	12	96	4	4:05
6 wt.%	282	18	94	6	3:30
8 wt.%	276	24	92	8	3:15
10 wt.%	270	30	90	10	3:05



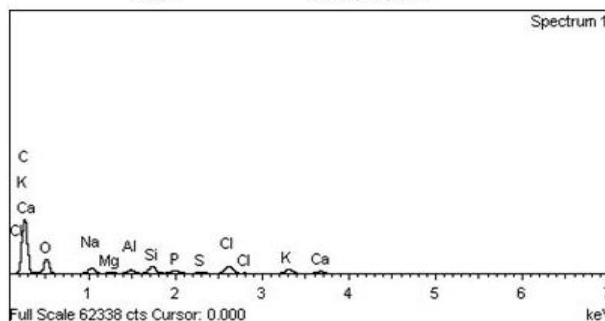
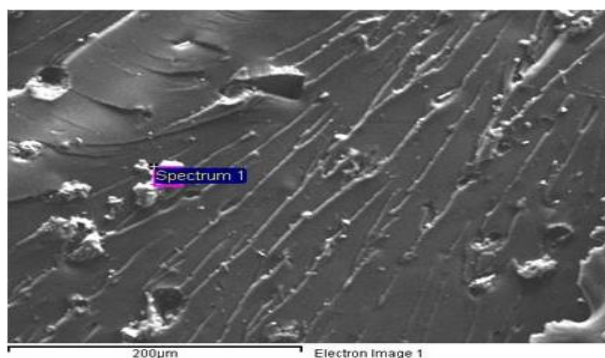
Fig. 2. Photographic representations of (a) NE test samples (b) 75 µm series EMSB test samples (c) <75 µm series EMSB test samples.



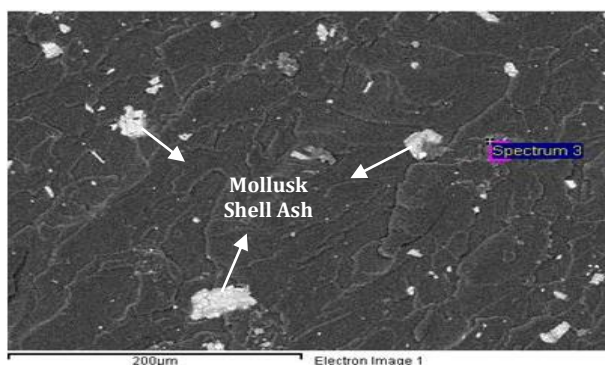
(a)

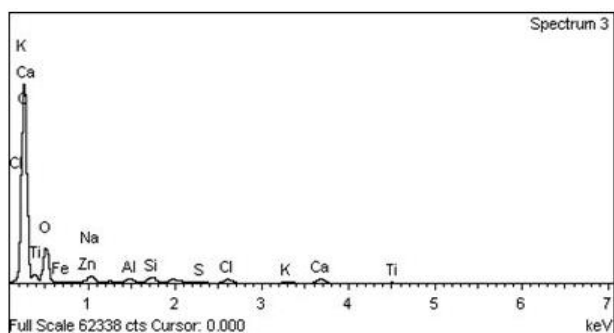


(b)



(c)





(d)

Fig. 3. (a) and (b) SEM/EDS results of the 75 μm 10 wt.% EMSB confirming the presence of Calcium (Ca), Carbon (C) and Oxygen (O) (CaCO_3) in the composite and (c) and (d) SEM/EDS results of the <75 μm 10 wt.% EMSB showing the dispersion of the filler within the composite and also confirming the presence of CaCO_3 along with other elements.

2.4 Determination of % Porosity

The porosity level of the developed EMSBs was evaluated dependent on the comparison between their theoretical and experimental densities using the expression in Equation 1. The theoretical density was evaluated based on the rule of mixture presented in Equation 2 and the experimental density was evaluated with the aid of a weighing balance and the formula presented in Equation 3.

$$\% \text{ Porosity} = ((\rho T - \rho Ex) \div \rho T) \times 100(\%) \quad (1)$$

Where, ρT and ρEx are the theoretical and experimental densities of the EMSBs, respectively.

$$\rho C = (Wf \times \rho E) + (Wf \times \rho P)(\text{g/cm}^3) \quad (2)$$

Where, ρC , ρE and ρP are the densities of the composites, epoxy and the MSA, respectively while W_f is the weight fraction of the composition.

The experimental density was evaluated using the expression presented in Equation 3.

$$\rho Ex = \frac{mC}{vC} (\text{g/cm}^3) \quad (3)$$

Where, ρEx , mC and vC are the experimental densities, mass and volume of the composites, respectively.

2.5 Wear Test

The wear test was conducted in compliance with ASTM D4060-14 standard [31]. The test samples

with disc-shaped geometries of 100 mm diameter and thickness of 6.35 mm were mounted to a turntable platform that rotates on a vertical axis at a fixed speed of 60 rpm. The turntable has dual abrading arms that are precision balanced. Each arm was loaded for 250 g pressure against the test samples and lowered onto the specimen surface. Characteristic rub-wear action is produced by contact of the test sample against the sliding rotation of the two abrading wheels. As the turntable rotates, the wheels are driven by the sample in opposite directions about a horizontal axis displaced tangentially from the axis of the sample. One abrading wheel robs the specimen outward toward the periphery and the other inward toward the center while a vacuum system removes the debris during the test. The test was conducted for 15 minutes for each test sample. The wheels traverse a complete circle on the specimen surface, revealing abrasion resistance at all angles relative to the weave or grain of the material. The resulting abrasion marks form a pattern of crossed arcs in a circular band that covers an area of approximately 30 cm^2 . The weight loss of the materials due to abrasion and their wear indices were evaluated using the relations in Equations 4 and 5 respectively. The experiment was carried out at room temperature of 24 ± 2 $^\circ\text{C}$. Five repeatability tests were conducted for each EMSB and their mean values were used in this study to ensure accuracy and reliability of test results.

Weight loss:

$$L = A - B \quad (4)$$

Where, L = weight loss in grammes and A and B are respective weights of test samples before and after abrasion in grammes.

Rate of wear:

$$I = \frac{A-B \times 1000}{C} (\text{mg/min}) \quad (5)$$

where, I = Taber Wear Index, A = Weight of test sample before abrasion in milligrammes, B = Weight of test sample after abrasion in milligrammes and C = number of test cycles in minutes.

2.6. Tensile test

The tensile test was performed in compliance with ASTM D638 standard [32]. The specimens'

overall length, gauge length, width and thickness are 115, 33, 10 and 5 ± 1 mm, respectively. The tensile test was performed using INSTRON 1195 universal testing machine at a fixed crosshead speed of 10 mm min^{-1} . The experiment was carried out at room temperature of 24 ± 2 °C. Five repeatability tests were conducted for each composite and their mean values were used in this study to ensure accuracy and reliability of test results.

2.7. Flexural test

The flexural test was performed in compliance with ASTM D790 standard [33]. The length, width and thickness of the specimen are 120, 12.7 and 3.2 mm, respectively. Correspondingly, the test was performed on an INSTRON universal testing machine. The test is stopped when the specimen reaches 5 % deflection or breaks before 5 % deflection. The experiment was carried out at room temperature of 24 ± 2 °C. Five repeatability tests were conducted for each composite and their mean values were used in this study to ensure accuracy and reliability of test results.

2.8. Scanning Electron Microscopy

The microstructural morphologies of the composites were studied using an AURIGA scanning electron microscope. The accelerating voltage of the microscope is 15 Kv.

3. RESULTS AND DISCUSSION

3.1. % Porosity

Figure 4 shows the variation of % porosity with filler loadings for the EMSBs. The void contents are significantly reduced at 4 and 6 wt.% filler loadings for both set of composites. However, the set of composites with smaller particle size exhibited a greater reduction in void contents except at 8 wt.% filler loading. This better performance can be attributed to the increased surface area of the MSA which in turn manifested in effective particulate-matrix bonding and high degree of compaction in the resultant composites, hence significant reduction in void contents.

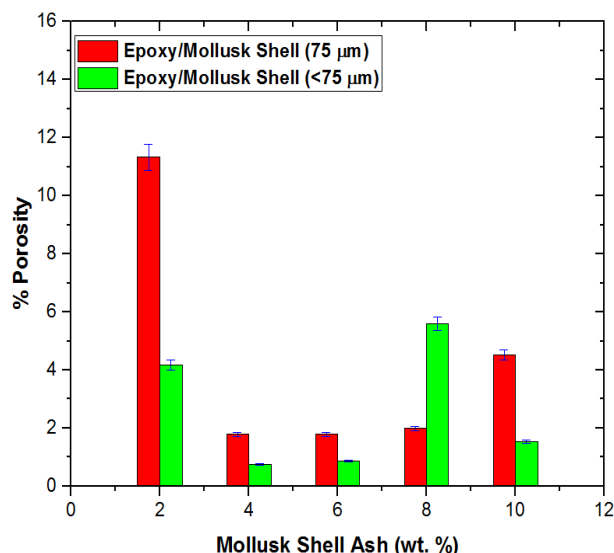


Fig. 4. Variation of % porosity with wt.% of MSA for the EMSBs.

3.2. Wear Behaviour

Figures 5 and 6 show the abrasion test results (weight loss and the wear indices) of the NE and EMSBs, respectively. Observations from these results revealed that, particle size and content of the filler are highly influential in enhancing the wear resistance of the composites. This is supported by the result where all the EMSBs filled with $<75 \mu\text{m}$ MSA outperformed their respective counterparts filled with $75 \mu\text{m}$ MSA.

The maximum enhancement was observed at 10 wt. % for the EMSBs filled with $<75 \mu\text{m}$ MSA. This EMSB has a wear index which is 92.45 % lower than that of the NE. The significant reduction in wear rate of this EMSB can be attributed to the high strength of interfacial adhesion between the epoxy matrix and MSA fillers which is due to increased surface area and surface energy of the particles.

In addition, the increase in degree of asperity on the surface topography of the EMSBs caused by the introduction of fillers into the epoxy matrix also enhanced the wear resistance of the materials; it is believed in this study, that the latter factor is the major enhancing mechanism for the EMSBs filled with $75 \mu\text{m}$ MSA, where it is believed that the strength of interfacial adhesion is fairly weak between the filler and the matrix as a result of reduction in surface area of the filler.

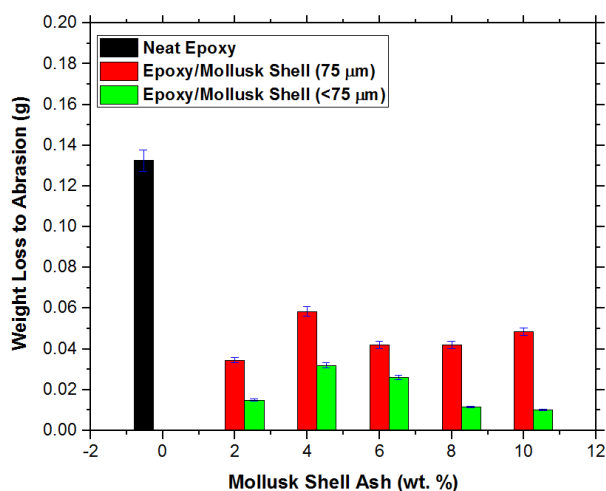


Fig. 5. Variation of % weight loss with wt.% of MSA for the NE and the EMSBs.

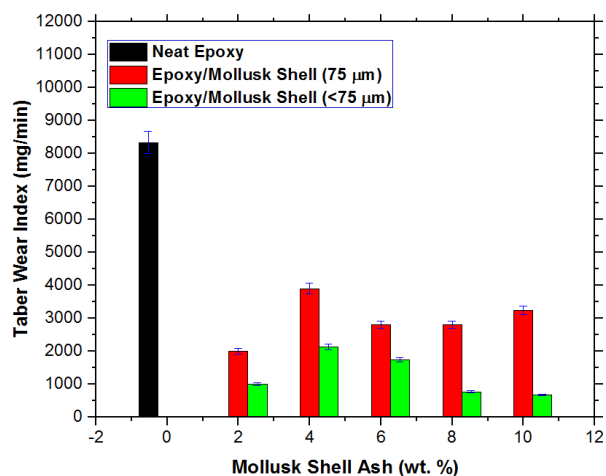


Fig. 6. Variation of Taber wear Index with wt.% of MSA for the NE and the EMSBs.

However, the results revealed that irrespective of particle size, the wear resistance of the composites was significantly enhanced which is a clear indication that the MSA which majorly comprises of CaCO₃ can be used to improve the wear resistance of epoxy resin.

Also, the inherent high wear resistance of snail shells and the presence of strengthening elements like nickel and manganese in large quantities in the snail shells as confirmed by the XRF result may also be responsible for this outstanding performance.

Similar improvement in wear properties of recycled low density polyethylene filled with varying particle sizes of snail shell has been reported by Atuanya and Aigbodion [34].

Their report showed reduction in wear rates of the composites with decreasing particle size and increase in filler loading. Also the work of Barman *et al.* [35] revealed an improvement in tribological properties of acrylonitrile-butadiene-styrene filled with micron-sized CaCO₃. Mimaroglu *et al.* [36] has also reported that high filler loading and smaller particle size of CaCO₃ significantly enhanced the wear resistance of glass fibre-reinforced unsaturated polyester. The findings of this research are in agreement with their observations.

3.3. Mechanical Behaviour

Figures 7 to 9 show the results of the tensile properties of the NE and the EMSBs.

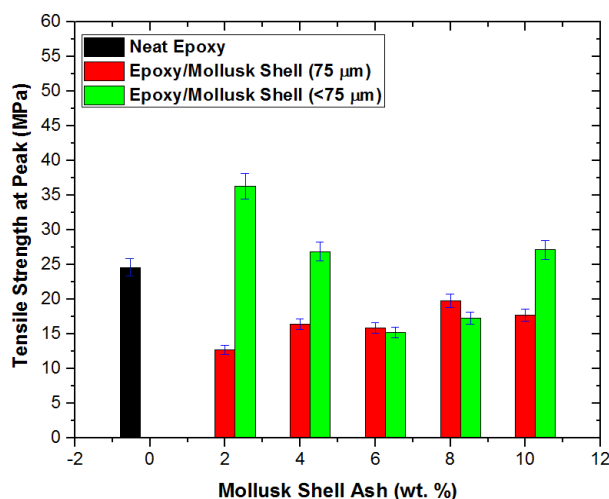


Fig. 7. Variation of tensile strength at peak with wt.% of MSA for the NE and the EMSBs.

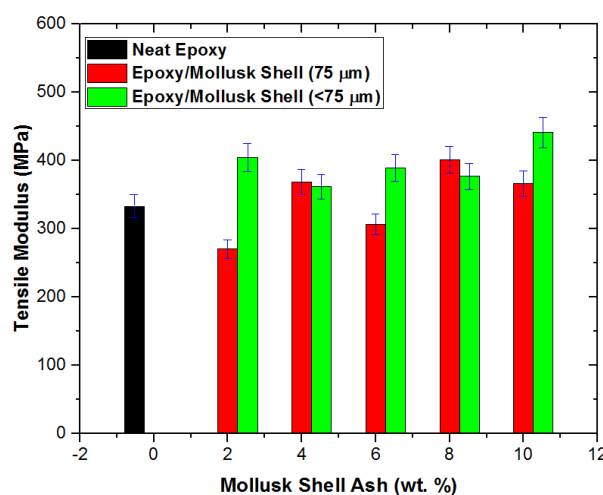


Fig. 8. Variation of tensile modulus with wt.% of MSA for the NE and the EMSBs.

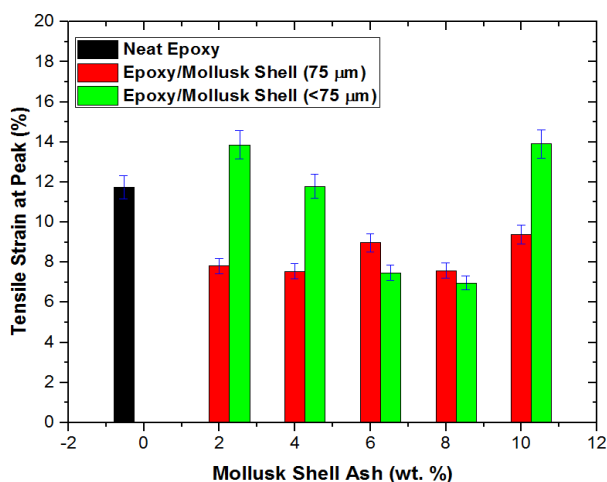


Fig. 9. Variation of tensile strain at peak with wt.% of MSA for the NE and EMSBs.

The mechanical properties of particulate-filled polymer composites have been markedly pointed out by *Fu et al.* [37] as highly dependent on the particle size, particle-matrix interfacial adhesion and particle content used in the composite system.

Figure 7 presents the result of the tensile strength at peak of the NE and the EMSBs. From the result it was revealed that the enhancement of tensile strength is dependent on the particle size of the filler, particle-matrix interfacial adhesion and particle loading. As shown by the result, nearly all the EMSBs filled with <75 μm MSA exhibited better tensile strengths at peak in comparison with the NE and the EMSBs filled with 75 μm MSA.

This occurrence of improved tensile strength with respect to particle size is a function of improved interfacial interaction between the surfaces of the MSA and the epoxy matrix and these results in an efficient stress transfer mechanism within the composite system. Effective stress transfer in filled-polymer composites is the key strengthening mechanism for tensile strength enhancement.

However, this strengthening mechanism becomes ineffective as the surface area of the particle is decreased as observed with the EMSBs filled with 75 μm MSA; this is because the strength of adhesion between the interfaces of the epoxy matrix and the MSA has been reduced.

Owing to this fact, the stress transfer within the composite becomes ineffective and this

increases with increasing filler content as the applied stress at this stage is principally bore by the epoxy matrix (the poorly bonded particles at this stage begin to debond from the epoxy matrix upon the application of stress) resulting in a composite with decreased tensile strength.

This explains why the 2 wt.% EMSB filled with <75 μm MSA gave the superlative tensile strength that is 32.19 % better than the NE and why no enhancement in tensile strength was given by the composites filled with 75 μm MSA. The work of Sadeghi and Esfandiari [38] on the effects of micro and nano CaCO₃ on the tensile strength of styrene butadiene styrene elastomer/CaCO₃ composite supports the findings of this research.

Figure 8 presents the result of the tensile moduli of the neat epoxy and the EMSBs. From the result it was observed that, the enhancement of tensile modulus is not dependent on the particle size but on particle loading. This is clearly seen with the trend of the result where there is an alternating increase and decrease in the moduli of both set of composites.

This occurrence can be viewed from an angle where the particle sizes selected for the present study are above the critical particle size where the particle size influences the modulus of the composite. In terms of particle loading, the superlative performances of both set of composites were observed at high filler contents; this was observed at 8 and 10 wt.% filler loadings for the EMSBs filled with 75 μm and <75 μm MSA, respectively. The moduli of these composites increased by 16.95 % and 24.43 %, respectively in comparison with that of the NE. The overall outstanding performance was given by the 10 wt.% EMSB filled with <75 μm MSA.

The occurrence of improved stiffness with corresponding increase in filler loading in particulate-filled polymer composites has been attributed to the fact that most inorganic fillers exhibit rigidity that is significantly higher than that of the polymer matrix. These observations are in agreement with the investigation of *Fu et al.* where they studied the effect of particle size on the tensile modulus of particulate-polymer composites [37,39].

The result of maximum tensile strain of the NE and the EMSBs is presented in Fig. 9. From this result, it was revealed that enhancement of ductility was favoured by smaller particle size. This enhancement is clearly seen at the lowest filler loading of 2 wt.% and at the highest filler loading of 10 wt.% for the EMSBs filled with <75 µm MSA.

It can be said that, the increase in the ductility of the composites at low filler loading is a function of better dispersion of the MSA within the epoxy matrix as there is enough matrix to bind the particles effectively, hence no serious aggregation of particles within the matrix.

Although, it has been established by researchers that the introduction of rigid fillers into polymer matrices practically leads to embrittlement of the composites once the critical filler loading is exceeded, the sudden increase observed in the ductility of the 10 wt.% EMSB filled with <75 µm MSA after a linear decrease from 4 to 8 wt.% filler loadings suggests that the plateau state of filler loading is either at 10 wt.% or has not yet been reached for this set of composites.

This sudden increase in ductility can be attributed to the combination of a very high strength of interfacial adhesion between the epoxy matrix and the MSA and absence of localized stress concentration in the resultant composite, hence a significant enhancement in the ductility of the material. The ductility of the 2 wt.% EMSB filled with <75 µm MSA outperformed that of the NE by 15.22 % while that of the 10 wt. % filled with the same particle superseded that of the NE by 15.47 %. The reduction in the ductility of the EMSBs filled with 75 µm MSA is as a result of filler-induced brittleness in the composite systems and the reduced surface areas of the particles which is favourable to formation of local network of MSA agglomerates within the composite system and particle debonding from the epoxy matrix. These two factors strongly hinder the enhancement of ductility in particulate-filled polymer composites.

A similar result was observed when Kamalbabu and Kumar [40] investigated the effect of particle size on the tensile properties of marine coral reinforced polymer composites.

Figures 10 and 11 show the flexural properties of the NE and the EMSBs.

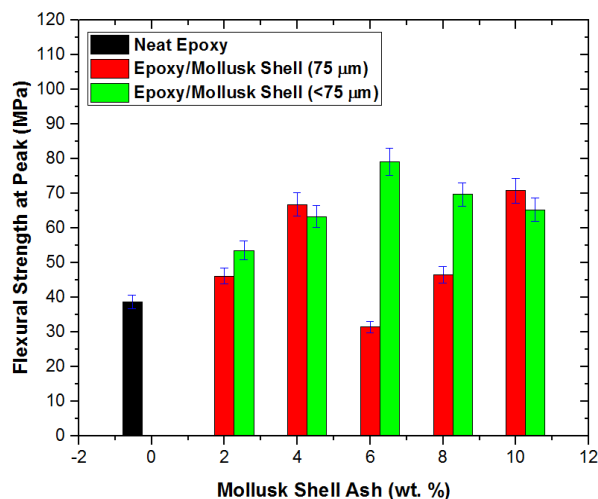


Fig. 10. Variation of Flexural Strength at Peak with wt. % of MSA for the NE and the EMSBs.

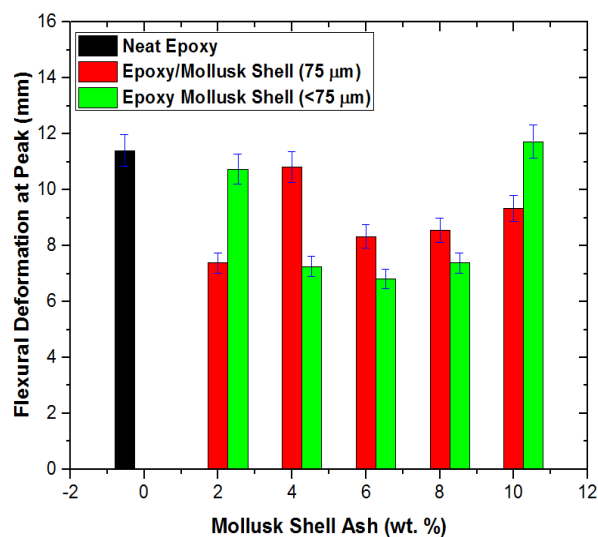


Fig. 11. Variation of flexural deformation at peak with wt. % of MSA for the NE and the EMSBs.

The result of the bending strength of the NE and the EMSBs is presented in Fig. 10. From the result, although only one of the composites showed no improvement in bending strength at peak, it is difficult to affirmatively state that this enhancement is dependent on particle size as there is an alternating rise and fall in the bending strengths at peak of both sets of composites based on particle size effect.

With respect to filler loading, the critical filler loading for the EMSBs filled with <75 µm MSA was clearly observed at 6 wt.% filler loading and for the EMSBs filled with 75 µm MSA it was indeterminate as there was no specific trend for the improvement in terms of filler loading. The superlative performance was demonstrated by the 6 wt.% EMSB filled with <75 µm MSA and in

comparison with the NE, a 51.09 % improvement in the bending strength at peak was observed.

Correspondingly, a 45.37 % improvement in bending strength at peak was given by the 10 wt.% ESMB filled with 75 μm MSA in comparison with that of the NE. This significant improvement in bending strength at peak can be attributed to most of the factors discussed under tensile properties of the composites.

The result of the flexural deformation at peak of the NE and the EMSBs is presented in Fig. 11. Observations from this result revealed that very low and very high wt. % of the MSA favoured the EMSBs filled with <75 μm MSA while intermediate filler loading ranging from 4-8 wt.% favoured the EMSBs filled with 75 μm MSA.

However, irrespective of particle size, this property was not significantly enhanced and this can be attributed to the nature of the test which does not allow for full transmission of applied load within the material system since it is more of a localized stress test.

The superlative flexural deformation at peak among the EMSBs filled <75 μm MSA was observed at 10 wt.% filler loading and for the EMSBs filled with 75 μm it was observed at 4 wt.% filler loading.

Figure 12 presents the energy absorbed to peak (toughness) for the NE and the EMSBs.

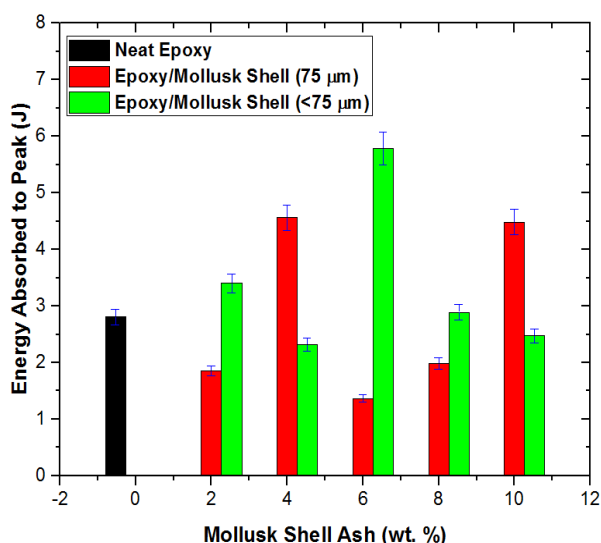


Fig. 12. Variation of energy absorbed to peak with wt.% of MSA for the NE and the EMSBs.

From the result, it is evident that the toughening of the composites is dependent on both particle size and content. For the materials to be toughened, the interparticle distance must be suitable to allow the interparticle matrix ligament lie in the plane stress state as this allows for easy plastic yield. This plastic yield increases with decreasing particle size and increasing filler content until the critical content is reached. Interparticle distance reduces with decreasing particle size and energy absorption potential of the material also increases with decreasing interparticle spacing.

It can be said that the 2 and 10 wt. % EMSBs filled with <75 μm MSA with improved toughness have suitable interparticle spacing that allows for improved plastic yield in the composite systems. In addition, increasing toughness in particulate-filled polymer composites is a function of crack pinning mechanism which is caused by the interaction between moving crack front and the second phase dispersion [41].

It is believed in this study that the second phase dispersion of the <75 μm MSA was even within epoxy at 2 wt. % filler loading and more connected networks of MSA were formed at 10 wt. % filler loading which resulted in abilities of these materials to effectively preclude rapid crack propagation via crack pinning mechanism. Additional energy is required by the cracks to break away from the pinned positions, hence improved in toughness of the materials. For the EMSBs filled with 75 μm MSA that showed no improvement in toughness, the interparticle spacing must have increased with increase in particle size and filler loading. Long interparticle distance allows the matrix ligament to lie in plane strain state where post-yield deformation of the matrix becomes difficult.

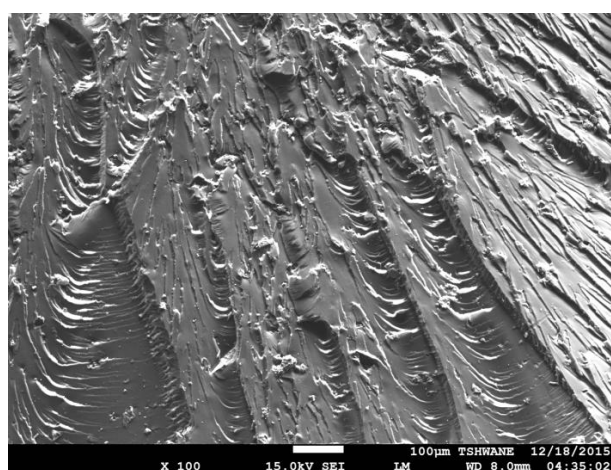
In addition, long interparticle distance will also result in formation of isolated large size agglomerates of MSA which serves as crack initiation sites that can trigger brittle behaviour in the material as crack pinning is now difficult. This limited post-yield deformation of the matrix together with weakened strength of interfacial adhesion in these composites will limit abilities to absorbed energy by localized shear yield deformation; hence their toughness cannot be improved. The conclusions reported by Zhang et

al. [42] on the effect of particle size and content of alumina on the toughness of high density polyethylene/alumina composites is in accord with these observations.

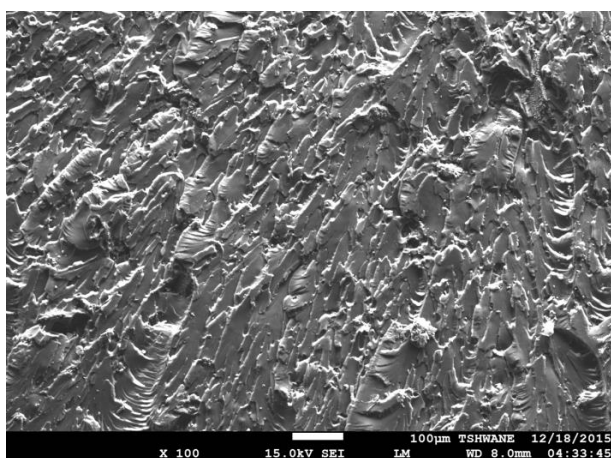
3.4. Fracture Behaviour

Figures 13 and 14 show the SEM images of the post-tensile test fractured surfaces of the representative samples of the EMSBs.

The 10 wt.% EMSBs for both sets of biocomposites were chosen as the representative samples for fractographic analysis. From these images, it was revealed that the EMSB filled with $75 \mu\text{m}$ MSA exhibited a rough fractured surface combined with fracture steps (Figs. 13 (b) and 14 (b)) and the EMSB filled with $75 \mu\text{m}$ MSA (Fig. 13 (a)) exhibited a combination of smooth (in from of grooves) and rough fractured surfaces.

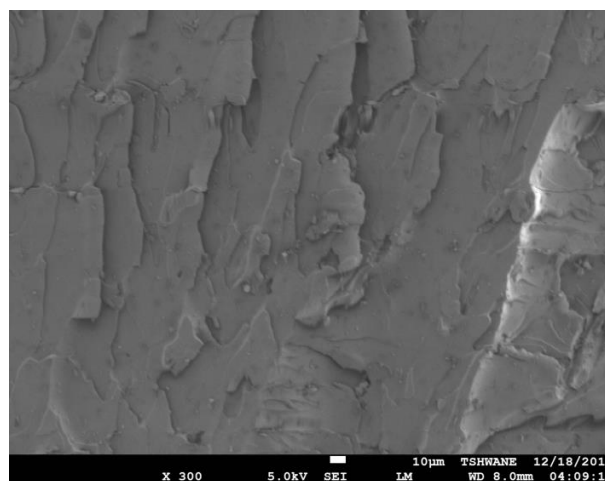


(a)

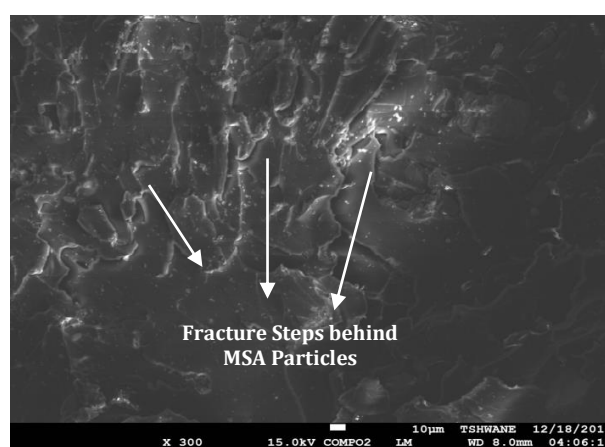


(b)

Fig. 13. (x100) SEM images of (a) Post-tensile test fractured surface of the 10 wt.% EMSB filled with $75 \mu\text{m}$ MSA (b) Post-tensile test fractured surface of the 10 wt.% EMSB filled with $<75 \mu\text{m}$ MSA.



(a)



(b)

Fig.14. (x300) SEM images of (a) Post-tensile test fractured surface of the 10 wt.% EMSB filled with $75 \mu\text{m}$ MSA (b) Post-tensile test fractured surface of the 10 wt.% EMSB filled with $<75 \mu\text{m}$ MSA showing fracture steps behind the MSA particles.

This is a clear indication that the EMSB filled with $<75 \mu\text{m}$ MSA underwent excessive post-yield deformation before the shear yielding of the epoxy matrix becomes predominant. This can be regarded as a ductile fracture which is due to effective crack pinning mechanism and the high strength of interfacial adhesion in the composite that are highly unfavorable to particle debonding. In (Fig. 14 (b)) fracture steps are shown behind the MSA particles indicating pinning mechanism before fracture [43].

As for the EMSB filled with $75 \mu\text{m}$ MSA, its fractured surface revealed an appreciable but not excessive plastic deformation before the material eventually failed in a quasibrittle manner. This brittle behaviour is facilitated by the presence of isolated large size agglomerates and weak interfaces in the composite. Isolated

large size agglomerates cannot serve as effective barriers to dislocation motion i.e. moving crack fronts (they serve as crack initiation sites) and weak interfaces do not resist crack propagation (they favour particle debonding). These observations are supported by the results of the tensile properties presented in Figs. 7 to 9 where nearly all the EMSBs filled with <75 µm MSA gave better tensile properties in comparison with their EMSBs counterparts filled with 75 µm MSA.

4. ENVIRONMENTAL IMPACT AND ECONOMIC ASSESSMENT

For the present investigation, 1000 shells of African land snails were used to produce the MSA fillers. This is a significant reduction in the volume of these shells which are usually regarded as waste, thereby constituting a major environmental nuisance in Nigeria. The 10 wt.% EMSB filled with <75 µm MSA used about 333 of these snail shells.

The consumption of epoxy resin for this composite was reduced by 10 % which is also 10 % reduction in cost of required epoxy resin. In addition, the improvement in aesthetic value of this composite without pigment addition, the absence of coupling agents and surface modification of the fillers equally contributed to the economic feasibility of its development.

5. CONCLUSION

The wear resistance and mechanical behaviour of EMSBs have been presented and investigated.

The findings of the present research have shown that addition of MSA to epoxy resin can improve the wear resistance and mechanical behavior of epoxy polymer matrix composites.

The optimum combination of wear and mechanical properties was given by the composite filled with 10 wt.% <75 µm MSA. Adding 10 wt.% <75 µm MSA to epoxy resin significantly reduced its wear index by 92.45 %.

The same composite showed 10.24 %, 32.33 %, 18.29 %, 31.02 %, 68.89 % and 2.83 % improvements in tensile strength, tensile modulus, tensile strain, absorbed energy,

flexural strength and flexural deformation, respectively.

Nonetheless, the addition of 2 wt.% <75 µm MSA to epoxy showed the superlative improvement in tensile properties and for the flexural properties this was observed with the composite filled with 6 wt.% of <75 µm MSA.

Although, particles of African land snail shell below 75 µm can present low-cost epoxy biocomposite with enhanced wear and mechanical properties, particles above this size are also effectively good in enhancing wear properties.

The observed properties have shown that EMSBs can be employed as potentially suitable engineering materials for structural applications such as bumpers of cars, keels of ships and contemporary interior household furniture.

REFERENCES

- [1] C. Brunel and A. Levinson, 'Measuring environmental regulatory stringency', *OECD Trade and Environment Working Papers*, 2013.
- [2] J. Sauvage, 'The stringency of environmental regulations and trade in environmental goods', *OECD Trade and Environment Working Papers*, 2014.
- [3] I.O. Oladele, J.L. Olajide and A.S. Ogunbadejo, 'The influence of chemical treatment on the mechanical behaviour of animal fibre-reinforced high density polyethylene composites', *American Journal of Engineering Research*, vol. 4, no. 2, pp. 19-26, 2015.
- [4] M. Zhan, R.P. Wool and J.Q. Xiao, 'Electrical properties of chicken feather fiber reinforced epoxy composites', *Composites, Part A: Applied Science and Manufacturing*, vol. 42, no. 3, pp. 229-233, 2011.
- [5] I.O. Oladele, J.L. Olajide, O.G. Agbabiaka and O.O. Akinwumi, 'Tensile properties and fractographic analysis of low density polyethylene composites reinforced with chemically modified keratin-based biofibres', *Journal of Minerals and Materials Characterization and Engineering*, vol. 3, pp. 344-352, 2015.
- [6] R.E. Njoku, A.E. Okon and T.C. Ikpaki, 'Effects of variation of particle size and weight fraction on the tensile strength and modulus of periwinkle shell reinforced polyester composite', *Nigerian Journal of Technology*, vol. 30, no. 2, pp. 88-92, 2012.

- [7] J.O. Agunsoye, S.A. Bello, I.S. Talabi, A.A. Yekinni, I.A. Raheem, A.D. Oderinde and T.E. Idegbekwu, 'Recycled aluminium cans/egg shell composites: evaluation of mechanical and wear properties', *Tribology in Industry*, vol. 37, no. 1, pp. 107-116, 2015.
- [8] S.B. Hassan, V.S. Aigbodion, and S.N. Patrick, 'Development of polyester/egg shell particulate composites', *Tribology in Industry*, vol. 34, no. 4, pp. 217-225, 2012.
- [9] F. Asuke, V.S. Aigbodion, M. Abdulwahab, O.S.I. Fayomi, A.P.I. Popoola, C.I. Nwoyi and B. Garba, 'Effects of bone particle on the properties and microstructure of polypropylene/bone ash particulate composites', *Results in Physics* 2, pp. 135-141, 2012.
- [10] I.O. Oladele, O.O. Daramola and A.T. Adewole, 'Comparative study of the reinforcement efficiency of cow bone and cow bone ash in polyester matrix composites for biomedical applications', *Acta Tehnica Corviniensis - Bulletin of Engineering Tome VII*, 2014.
- [11] P.H.F. Pereira, M. Rosa, M.O.H. Cioffi, K.C.C. Benini, A.C. Milanese, H.J.C. Voorwald and D.R. Mulinari, 'Vegetal fibers in polymeric composites: a review', *Polímeros*, vol. 25, no. 1, pp. 9-22, 2015.
- [12] I.A. Samotu, M. Dauda, F.O. Anafi and D.O. Obada, 'Suitability of recycled polyethylene/palm kernel shell-iron filings composite for automobile application', *Tribology in Industry*, vol. 37, no. 2, pp. 142-153, 2015.
- [13] T.B. Asafa, M.O. Durowoju, A.A. Oyewole, S.O. Solomon, R.M. Adegoke and O.J. Aremu, 'Potentials of snail shell as a reinforcement for discarded aluminum based materials', *International Journal of Advanced Science and Technology*, vol. 84, pp. 1-8, 2015.
- [14] Bourquin and R. Mayhew, Man and mollusc uses of shell-bearing molluscs - Past, present & future, available at: http://www.manandmollusc.net/advanced_uses/advanced_uses-print.html, accessed: 10.12.2015.
- [15] M.M. White, M. Chejlava, B. Fried and J. Sherma, 'The concentration of calcium carbonate in shells of freshwater snails', *American Malacological Bulletin*, vol. 22, no. 1, pp. 139-142, 2007.
- [16] C. Soído, M.C. Vasconcellos, A.G. Diniz and J. Pinheiro, 'An improvement of calcium determination technique in the shell of molluscs', *Brazilian Archives of Biology and Technology*, vol. 52, no. 1, pp. 93-98, 2009.
- [17] S.O. Adeosun S.O, E.I. Akpan and H.A. Akanegbu, 'Thermo-mechanical properties of unsaturated polyester reinforced with coconut and snail shells', *International Journal of Composite Materials*, vol. 5, no. 3, pp. 52-64, 2015.
- [18] C.I. Madueke, B. Bolasodun and R. Umunakwe, 'Mechanical properties of tere-phthalic unsaturated polyester resin reinforced with varying weight fractions of particulate snail shell', *IOSR Journal of Polymer and Textile Engineering*, vol. 1, no. 4, pp. 39-44, 2014.
- [19] G.C. Onuegbu and I.O. Igwe, 'The effects of filler contents and particle sizes on the mechanical and end-use properties of snail shell powder filled polypropylene', *Materials Sciences and Application*, vol.2, pp. 811-817, 2011.
- [20] S. Buranyi, Snail shells are inspiring tomorrow's toughest materials, available at: <http://motherboard.vice.com/read/the-amazing-snail-shell-science-inspiring-tomorrows-toughest-materials>, accessed: 10.12.2015.
- [21] Composites Resin Developments, Epoxy resin vs vinylester vs polyester use and application overview, available at: <http://www.compresdev.co.uk/CRD%20The%20Use%20and%20Application%20of%20Epoxy%20Resin%20vs%20Vinylester%20vs%20Polyester.pdf>, accessed: 10.12.2015
- [22] D.C. Gurit, Resin Comparison, available at: <http://www.netcomposites.com/guide-tools/guide/resin-systems/resin-comparison/>, accessed: 10.12.2015.
- [23] H.F. Mark, *Encyclopedia of polymer science and technology*. Hoboken: John Wiley and Sons, 2013.
- [24] G. Savage G, Composite materials technology in formula 1 motor racing, Honda racing F1, available at: <http://www.formula1dictionary.net/Big/Composite%20Materials%20Technology%20in%20Formula%201%20Motor%20Racing.pdf>, accessed: 10.12.2015.
- [25] G.C. Jacob, B. Hoevel, H.Q. Pham, M.L. Dettloff, N.E. Verghese, R.H. Turakhia and G. Hunter, Technical advances in epoxy technology for wind turbine blade composite fabrication, available at: <http://www.montana.edu/composites/documents/SAMPE%202007%20paper%20from%20DOW.pdf>, accessed: 10.12.2015.
- [26] AZO Materials, Composites in marine., available at, <http://www.azom.com/article.aspx?ArticleID=8155>, accessed: 10.12.2015

- [27] Mortensen, *Concise encyclopedia of composite materials*. Oxford, Elsevier, 2007.
- [28] C. Demerchant, Comparison of carbon fiber, kevlar (aramid) and E-glass used in composites for boatbuilding, available at: <http://www.christinedemerchant.com/carbon-kevlar-glass-comparison.html>, accessed: 10.12.2015.
- [29] T.A. Pearce, 'When a snail dies in the forest, how long will the shell persist? Effect of dissolution and micro-bioerosion', *American Malacological Bulletin*, vol. 26, pp. 111-117, 2008.
- [30] A. Hamilton-Amachree, H.D. Mepba and C.U. Ogunka-Nnoka, 'Mineral contents of tissues and body fluids and heavy metal contaminants of four predominant snail species in Niger Delta', *Journal of Food, Agriculture and Environment*, vol. 7, no. 2, pp. 163-168, 2009.
- [31] ASTM D4060-14: *Standard Test Method for Abrasion Resistance of Organic Coatings by the Taber Abraser*. ASTM International, West Conshohocken, PA, 2014.
- [32] ASTM D638-14: *Standard Test Method for Tensile Properties of Plastics*, ASTM International, West Conshohocken, PA, 2014.
- [33] ASTM D790-15e2: *Standard Test Method for Flexural Properties of Unreinforced and Reinforced Plastics and Electrical Insulating Materials*, ASTM International, West Conshohocken, PA, 2015.
- [34] C.O. Atuanya and V.S. Aigbodion, 'Effect of wear parameters on the wear behavior of recycled low density polyethylene/snail shell biocomposites', *Journal of Failure Analysis and Prevention*, vol. 14, no. 4, pp. 509-518, 2014.
- [35] T.K. Barman, J. Sudeepan, K. Kumarb and P. Sahoo, 'Study of tribological behavior of ABS/CaCO₃ composite using grey relational analysis', *Procedia Materials Science*, vol. 6, pp. 682 - 69, 2014.
- [36] A. Mimaroglu, M.G. Yilmaz and H. Unal, 'Study of the strength and erosive behavior of CaCO₃/glass fiber reinforced polyester composite', *Express Polymer Letters*, vol. 2, no. 12, pp. 890-895, 2008.
- [37] S. Fu, X. Feng, B. Lauke, and Y. Mai, 'Effects of particle size, particle/matrix interface adhesion and particle loading on mechanical properties of particulate-polymer composites', *Composites Part B*, vol. 39, pp. 933-961, 2008.
- [38] M. Sadeghi and A. Esfandiari, 'The effects of micro and nano CaCO₃ on the rheological and physico/mechanical behavior of an SBS/CaCO₃ composite', *Materials and Technology*, vol. 46, no. 6, pp. 695-703, 2012.
- [39] S. Bazhenov, *Mechanical behavior of filled thermoplastic polymers, metal, ceramic and polymeric composites for various uses*. John Cuppoletti (Ed.), Rijeka, InTech, 2011.
- [40] S. Zhang S, X.Y. Cao, Y.M. Ma, Y.C. Ke, J.K. Zhang and F.S. Wang, 'The effects of particle size and content on the thermal conductivity and mechanical properties of Al₂O₃/high density polyethylene (HDPE) composites', *Express Polymer Letters*, no.5, vol. 7, pp. 581-590, 2011.
- [41] P. Kamalbabu and G.C.M. Kumar, 'Effects of particle size on tensile properties of marine coral reinforced polymer composites', *Procedia Materials Science*, vol. 5, pp. 802-808, 2014.
- [42] Arencón D. and J.I. Velasco, 'Fracture toughness of polypropylene-based particulate composites', *Materials*, 2, pp. 2046-2094, 2009.
- [43] G.M. Newaz, *Microstructural Aspects of crack propagation in filled polymers: Fractography of modern engineering materials: Composite and metals*. ASTM STP 948. J.E. Masters and J.J. Au, (Eds.), Philadelphia: American Society for Testing and Materials, 1987.